ELSEVIER

Coordination Chemistry Reviews 230 (2002) 97–105

COORDINATION CHEMISTRY REVIEWS

www.elsevier.com/locate/ccr

Note

Ruthenium d-orbital delocalization in bis(bipyridine)ruthenium derivatives of redox active quinonoid ligands

S.I. Gorelsky, A.B.P. Lever *, Merhdad Ebadi

Department of Chemistry, York University, 4700 Keele Street, Toronto, Ont., Canada, M3J 1P3

Received 5 December 2001; accepted 8 March 2002

Contents

Abstract

Density Functional Theory (DFT) and INDO in the version developed by Zerner (ZINDO) are used to describe how the electronic coupling (π-back-donation etc.) in the series $[Ru(bpy)_2(LL)]^{2+}$ vary as a function of the coordinating atoms of LL. The bidentate ligand LL is *o*-benzoquinonediimine (NH·NH), and derivatives where one imino group is replaced by oxygen (NH·O) and by sulfur (NH·S). The electronic spectra of these species are calculated using both the INDO/S and time dependent DFRT models and compared with the experimental data. The agreement is excellent. The extent of interaction between the ruthenium dπ orbitals and LL increases in the sequence (NH·NH) < (NH·O) < (NH·S). It is noted that the semi-empirical ZINDO model provides a description of these molecules, which is quantitatively very similar to that derived from the more sophisticated DFT method.

Keywords: π-Back-donation; Electronic spectra; DFT; INDO; ZINDO; Time dependent DFRT; Ruthenium; Quinonediimine

1. Introduction

π-Back-donation is a major topic in coordination chemistry being used in a qualitative fashion to explain many observations in coordination chemistry from the stability of metal carbonyls to bond length variations in complexes where several supposedly π-accepting ligands vie for electron density off the metal center.

There have been many general studies of π-back-donation in a wide variety of systems using physical techniques such as NMR and vibrational spectra for comparison purposes. Systematic quantitative studies of such π-back-donation where a specific number is afforded to the property are rather rare. We have reported such data in a comparison of 2,2′-bipyridine (bpy), with 2,2′-bipyrazine (bpz) and with *o*-benzoquinonediimine (NH·NH, also called bqdi) [1] and also in series $[Ru(NH_3)_{6-2n}(LL)_n]^{2+}$ ($n = 1$–3) with the aforementioned ligands [2]. In this last example we wished to assess whether increasing the electron density on the ruthenium atom by replacing the weakly basic bidentate ligands, with ammonia residues, would allow additional electron density to be π-back-donated to the LL ligand. The π-back-donation was evaluated in terms of the percentage mixing of the Ru dπ orbital into the frontier π*-levels of the LL ligand. The redox active ligand *o*-benzoquinonediimine was seen to be a much better π-acceptor than the other two ligands, and was also shown

* Corresponding author. Tel.: +1-416-736-2100x22309; fax: +1-416-736-5936.
E-mail address: blever@yorku.ca (A.B.P. Lever).

0010-8545/02/$ - see front matter
PII: S0010-8545(02)00094-2

to be able to accommodate extra electron density when the central Ru was made more electron rich. *o*-Benzoquinonediimine is one of a family of members with various donor atoms where the =NH might be replaced by =O and =S. The question then arises as how the π-acceptor capability varies with these various donor ligands. We had generated the $[Ru(bpy)_2(O{\cdot}O)]^{2+}$ species electrochemically in 1986 [3] indicating then that *o*-benzoquinone (O·O) must be a very good π-acceptor. Bis(bipyridine)ruthenium complexes of aminophenol, (NH·O) [4] and aminothiophenol [5] have been reported but the dithiolene species $[Ru(bpy)_2(S{\cdot}S)]^{2+}$ is apparently unknown. These bis(bipyridine)ruthenium species are identified henceforth in this contribution by the donor set (NH·NH), (NH·O) etc.

In this contribution we also continue [6] our comparison of the use of density functional theory (DFT) versus semiempirical INDO/S method as implemented by Zerner et al. [7–12] (ZINDO) as a means of assessing π-back-donation quantitatively. Indeed DFT and the semiempirical INDO/S yield rather similar descriptions of electronic structure, the latter with little computational effort, relative to the former [6,13]. The INDO/S method gives excellent predictions of trends in electronic structure and good predictions of absolute band energies for visible region bands [1,2,6,14–40]. DFT [41] is proving itself to be a very useful and accurate method both to obtain geometries, electronic structure information, and reactivity e.g. applications to ruthenium complexes [6,42–67], and time-dependent density functional response theory (TD-DFRT) [68–70], is becoming very valuable as a means of predicting electronic spectra [6,29,60,71–83].The agreement between numbers derived from DFT (using the B3LYP functional with the LanL2DZ basis set) and from INDO/S are remarkably good save that the numbers derived from the latter for the (NH·S) ligand appear over-estimated if the DFT results are to be believed.

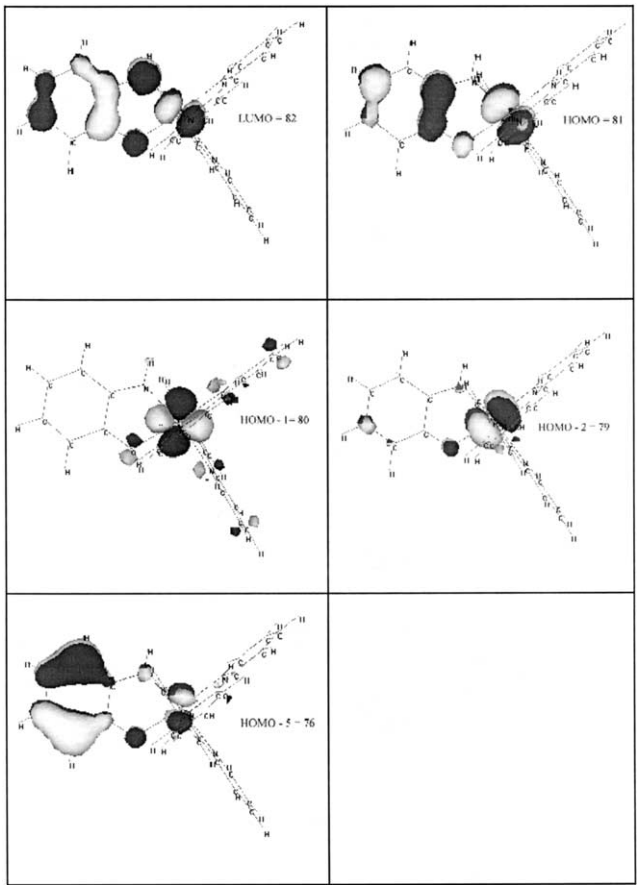

Fig. 1. Frontier molecular orbitals of $[Ru(bpy)_2(NH{\cdot}O)]^{2+}$ (INDO/S).

2. Computational details

The calculations presented in this article have been carried out using the GAUSSIAN 98 program [84]. Becke's three parameter hybrid functional [85] with the LYP correlation functional [86] (B3LYP) and an effective core potential basis set LanL2DZ [87–90] were employed in all the DFT calculations. The SCF convergence criterion was a change of less than 10^{-8} Hartree in the total energy [6]. Stabilities of DFT wavefunctions were tested with respect to relaxing spin constraints. Harmonic frequency calculations were performed to establish the nature of the critical points (minimum or transition state). The energies and intensities of the lowest 40 singlet–singlet electronic transitions were calculated with TD-DFRT. The atomic orbital compositions of molecular orbitals were calculated using Mulliken population analysis (MPA) and the AOMIX program [6,91a].

The INDO/S derived spectra and orbital mixing data are based on the aforementioned DFT optimized structures. These were obtained using the INDO/S method in the HYPERCHEM 5.1 program (Hypercube Inc., Florida), and incorporating the Ru INDO/S parameter set obtained by Krogh-Jespersen et al. [20]. Other atomic parameters were the default parameters of the Hyperchem program. The SCF convergence tolerance was 10^{-2} cal mol^{-1}. The number of singly excited configurations used was 1250 (e.g. 25 occupied and 25 virtual orbitals).

The absorption spectra profiles of the complexes were calculated using the SWIZARD program [6,91b]. The half-bandwidths of all electronic transitions, $\Delta_{1/2}$, were assumed to be equal 3000 cm^{-1} (a typical half-bandwidth value for the complexes under consideration).

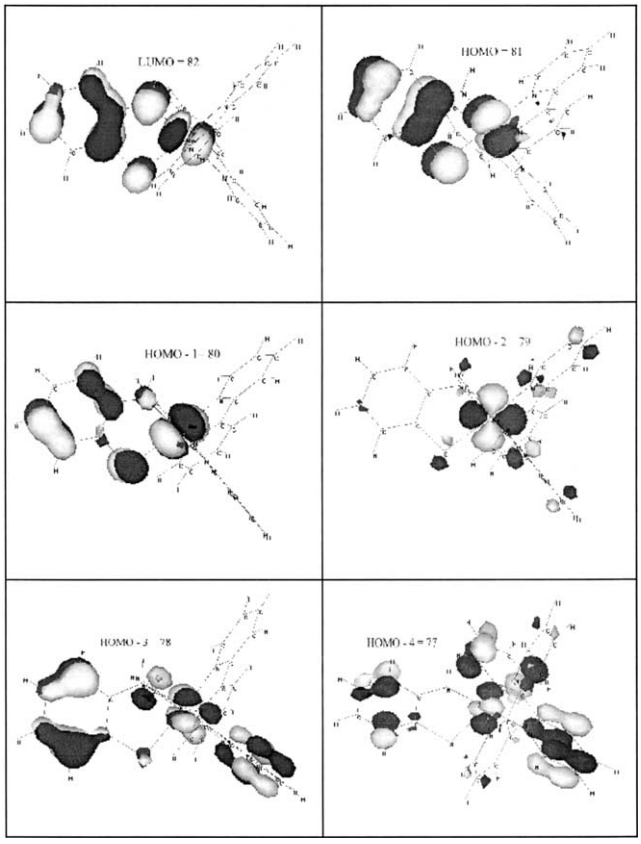

Fig. 2. Frontier molecular orbitals of $[Ru(bpy)_2(NH{\cdot}S)]^{2+}$ (INDO/S).

3. Results and discussion

The (NH·NH) species has been previously analyzed [1,2,6]. DFT Optimized geometries were obtained for other four closed shell [2+] or quinonoid oxidation level species, namely (NH·O), (NH·S), (O·O) and (S·S). The (O·O) and (S·S) species yielded a negative transition energy to the first spin triplet state implying that the ground state was actually not closed shell, but in fact was an open shell spin triplet. Re-optimization of the geometry as a spin triplet yielded a slightly lower energy structure in both these cases confirming the theoretical prediction that, at least for a gas phase structure, the spin triplet state was preferred. This result was predicted by both the INDO/S and DFT calculations. While the (S·S) species has never been reported experimentally, data for the (O·O) species with various groups substituting the *o*-benzoquinone ring (H, Cl_4 and di-*tert*-butyl) has been discussed [92] but these species were always studied in solution and never isolated. In an early study we [3] speculated that the canonical form Ru(III)-sq might make an important contribution to the otherwise presumed Ru(II)-q ground state. We had supposed a diamagnetic spin-coupled Ru(III)-sq description but now need to re-address this system experimentally. Solvent effects may yet cause stabilization of the spin singlet but given this uncertainty, the (O·O) and (S·S) species will not be considered in this Note.

Table 1
Orbital energies and atomic orbital contributions for frontier molecular orbitals of $[Ru(bpy)_2(LL)]^{2+}$ (INDO/S)

MO	Energy (eV)	Symmetry[a]	%Ru	%(NH·X)[b]	%(LL)	%(bpy)
[Ru(bpy)$_2$(NH·O)]$^{2+}$						
LUMO+2	−6.41	π*(bpy)	3	0, 0	0	97
LUMO+1	−6.54	π*(bpy)	4	0, 0	1	95
LUMO	−7.85	π*(NH·O)−d_{xz}	23	23, 10	72	5
HOMO	−12.93	d_{xz}+π*(NH·O)	53	0, 5	39	8
HOMO-1	−13.07	D_{xy}	74	2, 3	4	22
HOMO-2	−13.29	d_{yz}	76	2, 2	12	13
HOMO-3	−13.97	π(bpy)	2	0, 0	2	96
HOMO-4	−14.10	π(bpy)	1	0, 1	5	94
HOMO-5	−14.23	π(NH·O)+d_{xz}−d_{yz}	10	3, 5	82	10
[Ru(bpy)$_2$(NH·S)]$^{2+}$						
LUMO+2	−6.52	π*(bpy)	3	0, 0	0	97
LUMO+1	−6.66	π*(bpy)	3	0, 0	1	96
LUMO	−8.08	π*(NH·S)−d_{xz}	31	23, 8	64	5
HOMO	−13.07	d_{xz}+π*(NH·S)	45	0, 12	49	6
HOMO-1	−13.31	d_{yz}−π(NH·S)	58	3, 9	32	10
HOMO-2	−13.39	d_{xy}	73	2, 3	9	18
HOMO-3	−14.01	π(NH·S)+d_{xz}−d_{yz}	9	1, 5	36	55
HOMO-4	−14.11	π(bpy)	14	0, 3	27	59
HOMO-5	−14.21	π(bpy)	5	0, 0	6	89

[a] Ru–NH is the *x* coordinate, Ru–X is the *y* coordinate.

[b] Atomic orbital contributions from NH, X, respectively. Data for (NH·NH) have been published elsewhere [1,2,6]. A INDO/1 optimized geometry was used in refs [1,2] and DFT optimized in [6]. The overlap weighting factors in [1,2] differ slightly. As a consequence, the atomic orbital contributions for (NH·NH) also differ slightly in these three communications. The data in [6] are the most appropriate for comparison with the data here.

We restrict ourselves, therefore, in this paper to the (NH·O) and (NH·S) species and compare them with the previously discussed (NH·NH) species [1,2,6]. The key bond distances are shown in the appendix while CHIME readable structures may be found on our web site (see details at the end of the article). The bond distances fall within the expected ranges for species of this type (e.g. [93,94]) and the C–C distances alternate in the quinonoid rings as would be expected.

Figs. 1 and 2 show the INDO/S generated frontier molecular orbitals for the (NH·O) and (NH·S) species. Colour renditions of these MOs and those for the (NH·NH) species can be found on our web site. In the C_2 (NH·NH) species, the z axis bisects the quinonoid ligand and, with y perpendicular to the quinone plane, the t_{2g} set in O_h becomes the x^2-z^2, yz and xy orbitals which have σ (a), π (b) and δ (a) symmetry, respectively with respect to the quinonoid ligand. The Kohn–Sham orbitals of these species are very similar to the conventional MOs generated by INDO/S. However, the occupied d orbital sequence in the INDO/S calculations is not exactly the same as that in the DFT calculations, please see the footnotes to Table 2.

Table 2
Orbital energies and atomic orbital contributions for frontier molecular orbitals of $[Ru(bpy)_2(LL)]^{2+}$ (B3LYP/LanL2DZ)

MO	Energy (eV)	%Ru	%(NH·X)[a]	%(LL)	%(bpy)
[Ru(bpy)$_2$(NH·O)]$^{2+}$					
LUMO+2	−7.89	4	0, 0	0	96
LUMO+1	−8.03	4	0, 0	0	96
LUMO	−9.47	21	22, 13	75	4
HOMO[a]	−11.78	62	2, 8	29	9
HOMO-1	−11.85	65	3, 6	16	19
HOMO-2[a]	−12.20	59	1, 0	26	15
HOMO-3	−12.68	9	2, 2	35	56
HOMO-4[a]	−12.74	12	1, 2	33	55
HOMO-5[a]	−12.86	3	0, 0	5	92
[Ru(bpy)$_2$(NH·S)]$^{2+}$					
LUMO+2	−7.92	4	0, 0	0	96
LUMO+1	−8.07	3	0, 0	1	96
LUMO	−9.54	23	21, 19	73	4
HOMO[b]	−11.58	39	5, 25	57	4
HOMO-1[b]	−11.99	68	2, 8	12	20
HOMO-2[b]	−12.23	54	1, 1	32	14
HOMO-3	−12.58	35	2, 5	46	19
HOMO-4	−12.75	6	0, 0	3	91
HOMO-5	−12.88	2	0, 0	2	96

Data for X = S, O are provided here; data for (NH·NH) have been previously published [6]. Atomic orbital contributions from NH, X, respectively.

[a] The order of these molecular orbitals in DFT and INDO/S calculations is different. HOMO and HOMO-2, and HOMO-4 and HOMO-5 are interchanged.

[b] The order of these molecular orbitals in DFT and INDO/S calculations is different. HOMO (B3LYP) corresponds to HOMO-2 (INDO/S); HOMO-1 (B3LYP) corresponds to HOMO (INDO/S); HOMO-2 (B3LYP) corresponds to HOMO-1 (INDO/S).

Consideration of the molecular orbitals of this species leads one to conclude that they behave as though the molecule had C_{2v} symmetry in which these orbitals are orthogonal to one another and give rise to three d→π* (NH·NH) MLCT transitions. The spin-allowed dσ and dδ→π* transitions are very weak and occur at low energy near 11 000–13 000 cm^{-1} [6], while two fairly intense visible region absorption bands arise from both dπ→π* (NH·NH) and dπ→π* (bpy) MLCT. Mixing between the σ and δ orbitals, both of 'a' symmetry seems minimal.

While the (NH·X) species have no symmetry, consideration of the molecular orbitals shown in Figs. 1 and 2 reveals that it is still convenient to describe the orientation of d(t_{2g}) orbitals with respect to the quinonoid ligand. One orbital lies in the quinone plane, i.e. has σ-symmetry with respect thereto and the corresponding dσ→π* MLCT transition will be at low energy and very weak. We choose to define the Ru–NH axis as 'x' and Ru–O or S as 'y' with 'z' perpendicular to the quinonoid ligand. It is evident from Figs. 1 and 2 that in the frontier orbitals, which contain a significant d contribution, orbitals describable as d_{xy}, d_{xz}, d_{yz} and dδ can be discerned. Since the bite angle at the quinonoid ligand is not 90° (for (NH·O) it is 77.6°, for (NH·S) it is 81.7°), the defined x and y axes are not orthogonal and so these are not pure d orbitals but it is useful to describe them in this fashion. In particular the pπ orbital of S (or NH) is not orthogonal to d_{xz} (or d_{yz}) and, therefore, d_{xz} can overlap pπ(S) (and d_{yz} can overlap pπ(NH)).

Before discussing the assignments in more detail, we refer to Tables 1 and 2 which contain the atomic orbital contributions for the frontier orbitals of these species calculated from the INDO/S and DFT wavefunctions, respectively. Once again, despite the differences in the fundamentals of INDO/S and DFT, the orbital compositions are grossly similar. Fig. 3 compares the percent ruthenium contribution to the LUMO π*, i.e. the extent

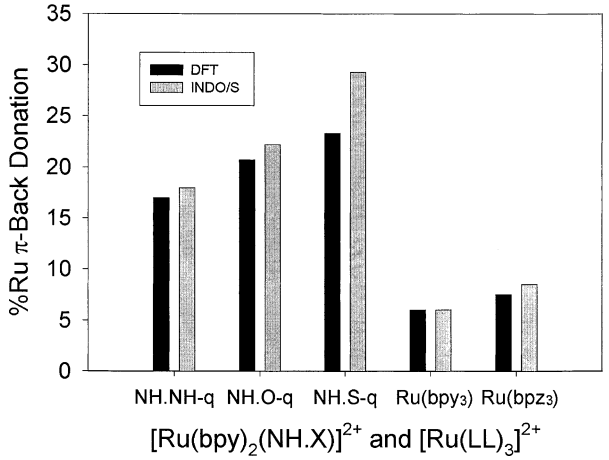

Fig. 3. Ruthenium character in the LUMO of $[Ru(bpy)_2(LL)]^{2+}$ (LL = NH·NH, NH·O, NH·S), in the LUMO+1,2 of $[Ru(bpy)_3]^{2+}$ and $[Ru(bpz)_3]^{2+}$.

of back-donation, which for all these species is significantly greater than for the $[Ru(bpy)_3]^{2+}$ and $[Ru(bpz)_3]^{2+}$ (bpz = 2,2′-bipyrazine) [6] ions also illustrated in Fig. 3. The extent of back-donation increases with the donor atom from $= N \ll NH < O < S$.

Considering the frontier orbitals in the (NH·O) species (Fig. 1) the HOMO (in INDO/S calculations or the HOMO-2 in DFT calculations) is d_{xz} which has a large contribution (39%) with the quinonoid π-system via binding to the pπ (O) orbital. The HOMO-1 is d_{xy} and as a consequence this is much a purer d orbital; it has some σ interaction with σ-orbitals of the quinonoid ligand. The HOMO-2 (in INDO/S calculations or the HOMO in DFT calculations) is mostly d_{yz}. The next lower MO which has substantial d character is HOMO-5 (INDO/S) or HOMO-4 (DFT) which involves a net bonding interaction with the free ligand fragment HOMO orbital having δ-symmetry in the corresponding (NH·NH) species. Bonding then occurs with a dδ orbital which can be described as mostly $(d_{yz} - d_{xz})$.

The situation with the (NH·S) complex is similar (Fig. 2) but the increased π-back-donation is accompanied by overall greater mixing between metal center and ligand such that more occupied frontier MOs have substantial d character (five for (NH·S) versus four for (NH·O)). The frontier orbitals can be described in the same fashion as for the (NH·O) species, though they lie in a slightly different energy order (Table 1). However there are now two δ-type metal orbitals (HOMO-3,4) both of which have substantial bipyridine π-character. For corresponding pairs of orbitals, e.g. HOMO-1 (NH·S) and HOMO-2 (NH·O) the molecular orbitals have larger d character in the less mixed (NH·O). Comparing the INDO/S and DFT calculations, the former may somewhat overestimate the extent of π-back donation in the (NH·S) species (Fig. 3).

Tables 1 and 2 also show the contributions of NH and X (X = O, S) fragments of the quinonoid ligand to the LUMO. These contributions represent a substantial fraction of the LUMO and it can be concluded that the electronic excitations from the three highest occupied MOs to the LUMO are largely internal to the metallocycle. This is consistent with earlier resonance Raman studies of related species [95] showing strong enhancement of Ru-NH modes but little enhancement of carbon ring localized vibrations.

Tables 3 and 4 show the predicted optical spectra derived from INDO/S and from TD-DFRT, respectively

Table 3
Electronic spectra of $[Ru(bpy)_2(LL)]^{2+}$ (INDO/S)

LL	Experimental spectrum [a]	Calculated spectrum [b]	Assignment [c]
NH·NH	13.3 (2.82)	10.2 {0.0045}	H(dδ) → L(π* LL)
		11.5 {0.0024}	H-2(dσ) → L(π* LL)
	19.4 (4.34) [2.6]	20.9 {0.65}	H-1(dπ) → L(π* LL)
	22.5 sh	23.9 {0.02}	H(dδ) → L+1(π* bpy)
		24.4 {0.04}	H-5(dπ),H-4 → L(π* LL)
		24.9 {0.12}	H-2(dσ) → L+1(π* bpy)
	30.9 sh	30.4 {0.20}	H-4(π-bpy) → L(π* LL)
		31.7 {0.08}	H-3(π-bpy) → L,L+1
		32.0 {0.13}	H-4(π-bpy) → L(π* LL)
		32.9 {0.12}	H(dδ) → L+4(π* bpy)
	35.6 (4.61)	33.9 {0.15}	H-2(dσ) → L+4(π* bpy)
		35.0 {0.22}	H-1(dπ) → L+3(π* bpy)
NH·O	n/a	8.2 {0.0006}	H-1(dσ) → L(π* LL) 82%
		9.4 {0.0049}	H-2(d_{yz}) → L(π* LL) 65%
	17.4 (4.1) [2.3]	18.1 {0.50}	H(d_{xz}) → L(π* LL) 69%
	20.5 (3.88)	22.4 {0.18}	H-5(dδ,π-LL) → L(π* LL) 78%
	23.0	24.5 {0.027}	H-1(dσ) → L+1(π* bpy) 52%; H(d_{xz}) → L+1(π* bpy) 28%
		25.4 {0.099}	H-1(dσ) → L+1(π* bpy) 28%; H-1(dσ) → L+2(π* bpy) 24%
NH·S	n/a	7.8 {0.0032}	H-2(dσ) → L(π* LL) 50%
		8.5 {0.0029)	H-1(d_{yz}) → L(π* LL) 47%; H-2(dσ) → L(π* LL) −39%
	19.3 (4.08) [3.3]	17.6 {0.27}	H(d_{xz}) → L(π* LL) 52%
		21.0 {0.55}	H-3(dδ,π LL) → L(π* LL) 28%; H-1(d_{yz}) → L(π* LL) 22%
	25.6 (3.24)	26.5 {0.063}	H-1(d_{yz}) → L+1(π* bpy) 25%; H-5(π bpy) → L(π* LL) −25%
	35.5 (4.55)	31.2 {0.17}	H-5(π bpy) → L+1 (π* bpy) 21%
		31.7 {0.46}	H-5(π bpy) → L+1 (π* bpy) 39%
		32.3 {0.17}	H-7(π LL) → L(π* LL) 62%

H, HOMO, H-1, HOMO-1, etc. L, LUMO, L+1, LUMO+1 etc.
[a] log ε (10^3 cm^{-1}) [halfbandwidth (10^3 cm^{-1})].
[b] Oscillator strength {10^3 cm^{-1}}.
[c] Only the major parent single-electron excitations are reported. Their percentage contributions to the wavefunctions of the excited states together with the signs are given in the table.

Table 4
Predicted Electronic spectra of $[Ru(bpy)_2(LL)]^{2+}$ (TD-DFRT)

LL	Calculated spectrum [a]	Assignment[b]
NH·NH	11.2 {0.0006}	H → L 72%
	13.0 {0.0010}	H-1 [c] → L 84%
	21.6 {0.11}	H → L+2 67%
	22.3 {0.20}	H-2 [c] → L 46%; H → L+2 24%
	24.4 {0.063}	H-1 [c] → L+1 90%
NH·O	9.2 {0.0005}	H → L 52%; H-1 → L −32%
	10.5 {0.0011}	H-1 → L 54%; H → L 22%
	19.5 {0.10}	H-2 → L 33%; H-3 → L −28%
	21.1 {0.089}	H-4 → L 70%
	21.5 {0.10}	H-3 → L 62%
	22.5 {0.026}	H-5 → L 90%
	23.4 {0.002}	H-1 → L+1 90%
	24.6 {0.0075}	H-1 → L+2 85%
	24.95 {0.056}	H-2 → L+2
NH·S	10.4 {0.0013}	H-1 → L 78%
	17.8 {0.028}	H-3 → L 52%; H-2 → L 19%
	20.3 {0.18}	H-2 → L 38%; H-4 → L −21%
	21.1 {0.048}	H-4 → L 71%
	22.4 {0.004}	H-1 → L+1 90%
	23.4 {0.004}	H-1 → L+2 90%
	25.5 {0.05}	H-2 → L+1 88%

See Table 3 for experimental data. Data for $[Ru(bpy)_2(NH·NH)]^{2+}$ has been published previously [6].

[a] Oscillator strength{10^3 cm^{-1}}.

[b] Only the major parent single-electron excitations are reported. Their percentage contributions to the wavefunctions of the excited states together with the signs are given.

[c] The order of these molecular orbitals in DFT and INDO/S calculations is different. HOMO (INDO/S) corresponds to HOMO-2 (B3LYP); HOMO (B3LYP) corresponds to HOMO-2 (INDO/S).

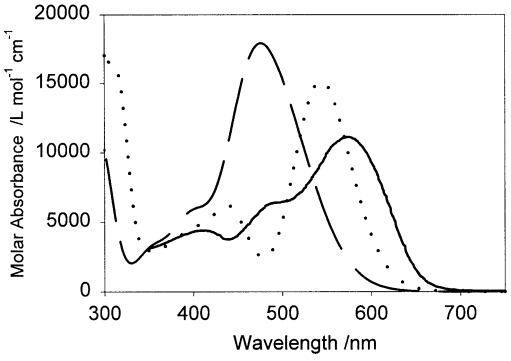

Fig. 4. Experimental (in CH_3CN) and predicted electronic spectra of $[Ru(bpy)_2(NH·O)]^{2+}$. Solid line—experimental; dotted line, TD-DFRT (B3LYP); hatched line, INDO/S. The intensities of electronic transitions from INDO/S calculations are reduced by a factor of 2.

with associated assignments for the (NH·O) and (NH·S) species; data for the (NH·NH) species have been previously discussed but are included here in more detail for completion and comparison. Figs. 4 and 5 provide the actual spectra of the (NH·X) species compared with the spectra predicted by INDO/S and by TD-DFRT (B3LYP) assuming bandwidths of 3000 cm^{-1} for all electronic transitions. The overall features of a strong lower energy feature and two weaker higher energy

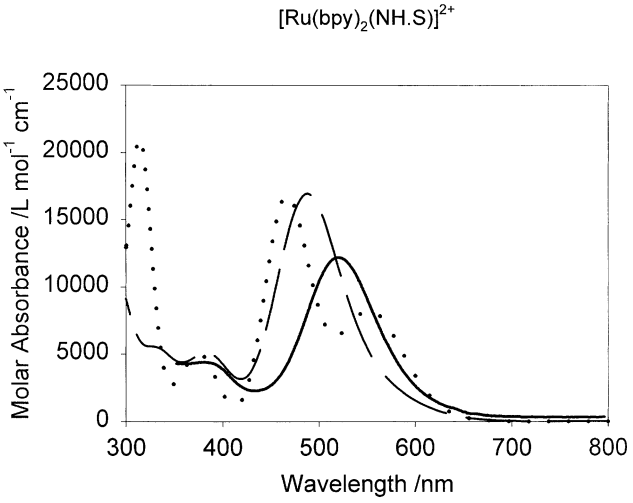

Fig. 5. Experimental (in CH_3CN) and predicted electronic spectra of $[Ru(bpy)_2(NH·S)]^{2+}$. Solid line—experimental; dotted line, TD-DFRT (B3LYP); hatched line, INDO/S. The intensities of electronic transitions from INDO/S calculations are reduced by a factor of 2.

features are well reproduced by both models. The assignments given in Tables 3 and 4 are similar to those for the (NH·NH) species except that the lower symmetry permits intensity to more than one d → π* (NH·X) transition. The INDO/S and TD-DFRT predictions are very similar but agreement with experimental band energies is better for INDO/S than for TD-DFRT. Both calculations are formally gas phase in nature and these are being compared with solution phase experimental data. The semi-empirical INDO/S parameters are derived from solution data and so generally provide somewhat better agreement with experiment.

The intense visible region transition contains d_{xz} → π*(LL) which parallels the dπ → π* (LL) transition in the (NH·NH) complex [6] and similar species. The overlap forbidden dσ → π*(LL) transition, of course, remains weak and at low energy. In the (NH·O) system, the transition from d_{yz} → π* (LUMO) is also at low energy and very weak presumably because it overlaps poorly with the LUMO resulting also in a small off-diagonal contribution to the energy. In the (NH·S) system, because of greater mixing between d orbitals and ligand, the d_{yz} → π* (LUMO) contributes both to a low energy weak transition and also to an intense visible region transition. An MLCT transition from the deeper dδ orbital to the LUMO, gains intensity in these low symmetry species compared with (NH·NH). In the (NH·O) species it is predicted to be weaker than the d_{xz} → π* (LUMO) transition and separated therefrom, to higher energy, by about 4000 cm^{-1}. Experimentally, these two transitions are resolved and separated by 3100 cm^{-1}. This transition has significant π–π* (NH·O) character according to the calculation. Indeed this π–π* contribution is confirmed by resonance Raman data collected earlier [95] when exciting into this electronic

transition. In the (NH·S) species it is actually predicted to be more intense than the $d_{xz} \rightarrow \pi^*$ (LUMO) and to be separated therefrom by 3300 cm^{-1} but experimentally, they are not resolved. Multiple $d \rightarrow \pi^*$ (bpy) MLCT transitions are seen beyond about 23 000 cm^{-1}.

4. Conclusions

Both the INDO/S and DFT models are successful in describing the electronic structure and electronic coupling in the $[Ru(bpy)_2(NH \cdot X)]^{2+}$ species (X = NH, O, S). The extent of interaction between the ruthenium center and the quinonoid ligand increases in the sequence just noted. This interaction is occurring both with the filled π-levels and the empty π* levels of the ligand.

The frontier Kohn–Sham orbitals of these species are very similar to the conventional MOs from INDO/S calculations.

Preliminary data for the, as yet, unknown $[Ru(bpy)_2(S \cdot S)]^{2+}$ species shows an even greater degree of coupling between metal center and dithiolene ligand.

5. Web page

Visit http://www.chem.yorku.ca/profs/lever and locate this paper in the Publications list for supporting information. This includes CHIME representations of the optimized geometries, colour renditions of the frontier molecular orbitals, and complete listing of MO information.

Acknowledgements

We are indebted to the Natural Sciences and Engineering Research Council for financial support. S.I. Gorelsky thanks the Province of Ontario for a Graduate Fellowship. We also thank the Johnson Matthey Company for the loan of ruthenium trichloride.

Appendix A: Bond distances (Å) in the DFT (B3LYP/LanL2DZ) optimized structures of $[Ru(bpy)_2(LL)]^{2+}$

Complex	Ru–N(bpy)$_{av}$	Ru–NH	Ru–X	C=X	C=NH
$[Ru(bpy)_2(NH \cdot O)]^{2+}$	2.10	2.00	2.10	1.31	1.34
$[Ru(bpy)_2(NH \cdot S)]^{2+}$	2.10	1.99	2.45	1.76	1.35
$[Ru(bpy)_2(NH \cdot NH)]^{2+}$	2.11	2.04			1.34

References

[1] S.I. Gorelsky, E.S. Dodsworth, A.B.P. Lever, A.A. Vlcek, Coord. Chem. Rev. 174 (1998) 469.
[2] A.B.P. Lever, S.I. Gorelsky, Coord. Chem. Rev. 208 (2000) 153.
[3] M. Haga, E.S. Dodsworth, A.B.P. Lever, Inorg. Chem. 25 (1986) 447.
[4] H. Masui, A.B.P. Lever, P.R. Auburn, Inorg. Chem. 30 (1991) 2402.
[5] M. Ebadi, A.B.P. Lever, Inorg. Chem. 38 (1999) 467.
[6] (a) S.I. Gorelsky, A.B.P. Lever, J. Organomet. Chem. 635 (2001) 187;
(b) S.I. Gorelski, Ph.D. Dissertation, York University, 2001.
[7] J. Ridley, M.C. Zerner, Theor. Chim. Acta 32 (1973) 111.
[8] J. Ridley, M.C. Zerner, Theor. Chim. Acta 42 (1976) 223.
[9] M.C. Zerner, G.H. Loew, R.F. Kirchner, U.T. Mueller-Westerhoff, J. Am. Chem. Soc. 102 (1980) 589.
[10] M.C. Zerner, in: N. Russo, D.R. Salahub (Eds.), Metal–Ligand Interactions, Kluwer Academic Publishers, Amsterdam, 1996, p. 493.
[11] M.C. Zerner, Metal–Ligand Interactions, Kluwer, The Netherlands, 1996, p. 493.
[12] C. Martin, M.C. Zerner, in: E.I. Solomon, A.B.P. Lever (Eds.), Inorganic Electronic Structure and Spectroscopy, vol. 1, Wiley, New York, 1999, p. 555.
[13] D.M. Ball, C. Buda, A.M. Gillespie, D.P. White, T.R. Cundari, Inorg. Chem. 41 (2002) 152.
[14] H. Masui, A.L. Freda, M.C. Zerner, A.B.P. Lever, Inorg. Chem. 39 (2000) 141.
[15] R.A. Metcalfe, A.B.P. Lever, Inorg. Chem. 36 (1997) 4762.
[16] A.D. Bacon, M.C. Zerner, Theor. Chim. Acta 53 (1979) 21.
[17] J.D. Baker, M.C. Zerner, Chem. Phys. Lett. 175 (1990) 192.
[18] J.D. Baker, M.C. Zerner, J. Phys. Chem. 95 (1991) 8614.
[19] M.G. Cory, M.C. Zerner, Chem. Rev. 91 (1991) 813.
[20] K. Krogh-Jespersen, J.D. Westbrook, J.A. Potenza, H.J. Schugar, J. Am. Chem. Soc. 109 (1987) 7025.
[21] K. Krogh-Jespersen, X. Zhang, J.D. Westbrook, R. Fikar, K. Nayak, W.-L. Kwik, J.A. Potenza, H.J. Schugar, J. Am. Chem. Soc. 111 (1989) 4082.
[22] K. Krogh-Jespersen, X. Zhang, Y. Ding, J.D. Westbrook, J.A. Potenza, H.J. Schugar, J. Am. Chem. Soc. 114 (1992) 4345.
[23] I.A. Bagatin, H.E. Toma, Transition Met. Chem. (Dordrecht Neth.) 25 (2000) 686.
[24] A.M. Barthram, M.D. Ward, New J. Chem. 24 (2000) 501.
[25] V.R.L. Constantino, H.E. Toma, L.F.C. de Oliveira, F.N. Rein, R.C. Rocha, D. de Oliveira Silva, J. Chem. Soc. Dalton Trans. (1999) 1735.
[26] C.J. Da Cunha, E.S. Dodsworth, M.A. Monteiro, A.B.P. Lever, Inorg. Chem. 38 (1999) 5399.

[27] R.A. Metcalfe, L.C.G. Vasconcellos, H. Mirza, D.W. Franco, A.B.P. Lever, J. Chem. Soc. Dalton Trans. (1999) 2653.
[28] M.F. Ryan, R.A. Metcalfe, A.B.P. Lever, M. Haga, J. Chem. Soc. Dalton (2000) 2357.
[29] R.S. da Silva, S.I. Gorelsky, E.S. Dodsworth, E. Tfouni, A.B.P. Lever, J. Chem. Soc. Dalton Trans. (2000) 4078.
[30] W.K. Seok, S.B. Yim, H.N. Lee, T.M. Klapotke, Z. Naturforsch. B: Chem. Sci. 55 (2000) 462.
[31] W.K. Seok, S.B. Yim, T.M. Klapotke, P.S. White, J. Organomet. Chem. 559 (1998) 165.
[32] Y.K. Shin, B.S. Brunschwig, C. Creutz, M.D. Newton, N. Sutin, J. Phys. Chem. 100 (1996) 1104.
[33] M.D. Ward, Inorg. Chem. 35 (1996) 1712.
[34] Y.K. Shin, B.S. Brunschwig, C. Creutz, N. Sutin, J. Am. Chem. Soc. 117 (1995) 8668.
[35] Y.K. Shin, D.J. Szalda, B.S. Brunschwig, C. Creutz, N. Sutin, Inorg. Chem. 36 (1997) 3190.
[36] A.Y. Ershov, O.V. Sizova, A.D. Shashko, N.V. Ivanova, A.B. Nikol'skii, Russ. J. Gen. Chem. 70 (2000) 846.
[37] O.V. Sizova, V.I. Baranovskii, N.V. Ivanova, A.I. Panin, Russ. J. Coord. Chem. 24 (1998) 219.
[38] O.V. Sizova, V.I. Baranovskii, A.I. Panin, N.V. Ivanova, J. Struct. Chem. 39 (1999) 471.
[39] O.V. Sizova, N.V. Ivanova, A.B. Nikol'skii, A.I. Panin, V.I. Baranovskii, A.Y. Ershov, Russ. J. Gen. Chem. 69 (1999) 576.
[40] M.K. Nazeeruddin, S.M. Zakeeruddin, R. Humphry-Baker, S.I. Gorelsky, A.B.P. Lever, M. Gratzel, Coord. Chem. Rev. 208 (2000) 213.
[41] J. Li, L. Noodleman, D.A. Case, in: E.I. Solomon, A.B.P. Lever (Eds.), Inorganic Electronic Structure and Spectroscopy, vol. 1, 1999, p. 661.
[42] G. Albano, P. Belser, C. Daul, Inorg. Chem. 40 (2001) 1408.
[43] F. Bernardi, A. Bottoni, G.P. Miscione, Organometallics 19 (2000) 5529.
[44] P. Boulet, M. Buchs, H. Chermette, C. Daul, E. Furet, F. Gilardoni, F. Rogemond, C.W. Schlaepfer, J. Weber, J. Phys. Chem. A 105 (2001) 8999.
[45] P. Boulet, M. Buchs, H. Chermette, C. Daul, F. Gilardoni, F. Rogemond, C.W. Schlaepfer, J. Webe, J. Phys. Chem. A 105 (2001) 8991.
[46] M. Buchs, C. Daul, Chimia 52 (1998) 163.
[47] J.N.I. Coalter, G.J. Spivak, H. Gerard, E. Clot, E.R. Davidson, O. Eisenstein, K.G. Caulton, J. Am. Chem. Soc. 120 (1998) 9388.
[48] C. Daul, E.J. Baerends, P. Vernooijs, Inorg. Chem. 33 (1994) 3538.
[49] N. Dolker, G. Frenking, J. Organomet. Chem. 617–618 (2001) 225.
[50] D.J. Dooling, R.J. Nielsen, L.J. Broadbelt, Chem. Eng. Sci. 54 (1999) 3399.
[51] F. Gilardoni, J. Weber, A. Hauser, C. Daul, J. Comput. Chem. 20 (1999) 1343.
[52] S.I. Gorelsky, S.C. da Silva, A.B.P. Lever, D.W. Franco, Inorg. Chim. Acta 300-302 (2000) 698.
[53] M. Harada, H. Dexpert, J. Phys. Chem. 100 (1996) 565.
[54] E.N.-M. Ho, Z. Lin, W.-T. Wong, Eur. J. Inorg. Chem. (2001) 1321.
[55] C. Kim, I. Novozhilova, M.S. Goodman, K.A. Bagley, P. Coppens, Inorg. Chem. 39 (2000) 5791.
[56] T. Matsubara, Organometallics 20 (2001) 19.
[57] T. Matsubara, N. Koga, D.G. Musaev, K. Morokuma, Organometallics 19 (2000) 2318.
[58] J.E. McGrady, Angew. Chem. Int. Ed. 39 (2000) 3077.
[59] J.E. McGrady, T. Lovell, R. Stranger, M.G. Humphrey, Organometallics 16 (1997) 4004.
[60] J.E. Monat, J.H. Rodriquez, J.K. McCusker, Abstracts of Papers, 222nd ACS National Meeting, Chicago, IL, United States, 26–30 August, 2001 p. INOR486.
[61] I.J. Munslow, K.M. Gillespie, R.J. Deeth, P. Scott, Chem. Commun. (Cambridge, UK) (2001) 1638.
[62] Y. Musashi, S. Sakaki, J. Am. Chem. Soc. 122 (2000) 3867.
[63] P.M. Nave, M. Draganjac, B. Ward, A.W. Cordes, T.M. Barclay, T.R. Cundari, J.J. Carbo, F. Maseras, Inorg. Chim. Acta 316 (2001) 13.
[64] G.B. Richter-Addo, R.A. Wheeler, C.A. Hixson, L. Chen, M.A. Khan, M.K. Ellison, C.E. Schulz, W.R. Scheidt, J. Am. Chem. Soc. 123 (2001) 6314.
[65] M. Stener, M. Calligaris, THEOCHEM 497 (2000) 91.
[66] S.Y. Yang, T.B. Wen, G. Jia, Z. Lin, Organometallics 19 (2000) 5477.
[67] I.S. Zavarine, C.P. Kubiak, T. Yamaguchi, K. Ota, T. Matsui, T. Ito, Inorg. Chem. 39 (2000) 2696.
[68] E.K.U. Gross, W. Kohn, Adv. Quantum Chem. 21 (1990) 255.
[69] E.K.U. Gross, C.A. Ullrich, U.J. Gossmann, NATO ASI Ser. Ser. B 337 (1995) 149.
[70] G. Vignale, Int. J. Mod. Phys. B 15 (2001) 1714.
[71] W.B. Euler, M. Cheng, C. Zhao, Polyhedron 20 (2001) 507.
[72] S.I. Gorelsky, A.B.P. Lever, Int. J. Quantum Chem. 80 (2000) 636.
[73] (a) M. Turki, C. Daniel, S. Záliš, A. Vlček Jr., J. van Slageren, I.R. Farrel, F. Hartl, S. Záliš, T.A. Mahabiersing, J. Chem. Soc. Dalton Trans. (2000) 4323;
(b) M. Turki, C. Daniel, S. Záliš, A. Vlček, Jr., J. van Slageren, D.J. Stufkens, J. Am. Chem. Soc. 123 (2001) 11431.
[74] I.R. Farrell, J. van Slageren, S. Záliš, A. Vlček, Jr., Inorg. Chim. Acta 315 (2001) 44.
[75] S.J.A. van Gisbergen, J.A. Groeneveld, A. Rosa, J.G. Snijders, E.J. Baerends, J. Phys. Chem. A 103 (1999) 6835.
[76] K. Wakamatsu, K. Nishimoto, T. Shibahara, Inorg. Chem. Commun. 3 (2001) 677.
[77] S. Záliš, H. Stoll, E.J. Baerends, W. Kaim, Inorg. Chem. 38 (1999) 6101.
[78] S. Reinartz, M.-H. Baik, P.S. White, M. Brookhart, J.L. Templeton, Inorg. Chem. 40 (2001) 4726.
[79] C.A. Grapperhaus, E. Bill, T. Weyhermüller, F. Neese, K. Wieghardt, Inorg. Chem. 40 (2001) 4191.
[80] A. Rosa, E.J. Baerends, S.J.A. van Gisbergen, E. van Lenthe, J.A. Groeneveld, J.G. Snijders, J. Am. Chem. Soc. 121 (1999) 10356.
[81] M. Glöckle, W. Kaim, A. Klein, E. Roduner, G. Hübner, S. Zalis, J. van Slageren, F. Renz, P. Gütlich, Inorg. Chem. 40 (2001) 2256.
[82] M.J. Calhorda, G.B. Drew, L.P. Felix, C.A. Fonseca, S.S. Gamelas, M.C. Godinho, I.S. Goncalves, E. Hunstock, J.P. Lopes, P.A. Jorge, F. Pina, C.C. Romao, A. Gil Santos, J. Organomet. Chem. 632 (2001) 94.
[83] G. Ricciardi, A. Rosa, E.J. Baerends, J. Phys. Chem. A. 105 (2001) 5242.
[84] M.J. Frisch, G.W. Trucks, H.B. Schlegel, G.E. Scuseria, M.A. Robb, J.R. Cheeseman, V.G. Zakrzewski, J.A. Montgomery, Jr., R.E. Stratmann, J.C. Burant, S. Dapprich, J.M. Millam, A.D. Daniels, K.N. Kudin, M.C. Strain, O. Farkas, J. Tomasi, V. Barone, M. Cossi, R. Cammi, B. Mennucci, C. Pomelli, C. Adamo, S. Clifford, J. Ochterski, G.A. Petersson, P.Y. Ayala, Q. Cui, K. Morokuma, D.K. Malick, A.D. Rabuck, K. Raghavachari, J.B. Foresman, J. Cioslowski, J.V. Ortiz, B.B. Stefanov, G. Liu, A. Liashenko, P. Piskorz, I. Komaromi, R. Gomperts, R.L. Martin, D.J. Fox, T. Keith, M.A. Al-Laham, C.Y. Peng, A. Nanayakkara, C. Gonzalez, M. Challacombe, P.M.W. Gill, B. Johnson, W. Chen, M.W. Wong, J.L. Andres, C. Gonzalez, M. Head-Gordon, E.S. Replogle, J.A. Pople, GAUSSIAN-98, Revision A.7, Gaussian, Inc, Pittsburgh PA, 1998.
[85] A.D. Becke, J. Chem. Phys. 98 (1993) 5648.
[86] C. Lee, W. Yang, R.G. Parr, Phys. Rev. B 37 (1988) 785.
[87] T.H. Dunning, Jr., P.J. Hay, in: H.F. Schaefer, III (Ed.), Modern Theoretical Chemistry, vol. 3, Plenum, New York, 1976, p. 1.

[88] P.J. Hay, W.R. Wadt, J. Chem. Phys. 82 (1985) 270.
[89] P.J. Hay, W.R. Wadt, J. Chem. Phys. 82 (1985) 284.
[90] P.J. Hay, W.R. Wadt, J. Chem. Phys. 82 (1985) 299.
[91] (a) S.I. Gorelsky, A.B.P. Lever, AOMIX Program, Revision 4.7 (available at http://www.obbligato.com/software/aomix/);
(b) S.I. Gorelsky, SWIZARD Program, Revision 1 (available at http://www.obbligato.com/software/swizard).
[92] H. Masui, E.S. Dodsworth, A.B.P. Lever, Inorg. Chem. 32 (1993) 258.
[93] O. Carugo, C.B. Castellani, K. Djinovic, M. Rizzi, J. Chem. Soc. Dalton Trans. (1992) 837.
[94] O. Carugo, K. Djinovic, M. Rizzi, C. Bisi Castellani, J. Chem. Soc. Dalton Trans. (1991) 1255.
[95] A.B.P. Lever, H. Masui, R.A. Metcalfe, D.J. Stufkens, E.S. Dodsworth, P.R. Auburn, Coord. Chem. Rev. 125 (1993) 317.